ARTICLE

doi:10.1038/nature12744

Therapeutic efficacy of potent neutralizing HIV-1-specific monoclonal antibodies in SHIV-infected rhesus monkeys

Dan H. Barouch[1,2], James B. Whitney[1], Brian Moldt[3], Florian Klein[4], Thiago Y. Oliveira[4], Jinyan Liu[1], Kathryn E. Stephenson[1], Hui-Wen Chang[1], Karthik Shekhar[5], Sanjana Gupta[5], Joseph P. Nkolola[1], Michael S. Seaman[1], Kaitlin M. Smith[1], Erica N. Borducchi[1], Crystal Cabral[1], Jeffrey Y. Smith[1], Stephen Blackmore[1], Srisowmya Sanisetty[1], James R. Perry[1], Matthew Beck[6], Mark G. Lewis[7], William Rinaldi[8], Arup K. Chakraborty[2,5], Pascal Poignard[3], Michel C. Nussenzweig[4,9]* & Dennis R. Burton[2,3]*

Human immunodeficiency virus type 1 (HIV-1)-specific monoclonal antibodies with extraordinary potency and breadth have recently been described. In humanized mice, combinations of monoclonal antibodies have been shown to suppress viraemia, but the therapeutic potential of these monoclonal antibodies has not yet been evaluated in primates with an intact immune system. Here we show that administration of a cocktail of HIV-1-specific monoclonal antibodies, as well as the single glycan-dependent monoclonal antibody PGT121, resulted in a rapid and precipitous decline of plasma viraemia to undetectable levels in rhesus monkeys chronically infected with the pathogenic simian-human immunodeficiency virus SHIV-SF162P3. A single monoclonal antibody infusion afforded up to a 3.1 log decline of plasma viral RNA in 7 days and also reduced proviral DNA in peripheral blood, gastrointestinal mucosa and lymph nodes without the development of viral resistance. Moreover, after monoclonal antibody administration, host Gag-specific T-lymphocyte responses showed improved functionality. Virus rebounded in most animals after a median of 56 days when serum monoclonal antibody titres had declined to undetectable levels, although, notably, a subset of animals maintained long-term virological control in the absence of further monoclonal antibody infusions. These data demonstrate a profound therapeutic effect of potent neutralizing HIV-1-specific monoclonal antibodies in SHIV-infected rhesus monkeys as well as an impact on host immune responses. Our findings strongly encourage the investigation of monoclonal antibody therapy for HIV-1 in humans.

A series of broad and potent HIV-1 Env-specific monoclonal antibodies have recently been isolated[1,2] and have been shown to target the CD4 binding site[3–7], the V1/V2 loops[8,9], the V3/V4 loops and N332 glycans[10–13], and the membrane proximal external region[14]. Previous studies in humanized mice and humans using the earlier generation of HIV-1 Env-specific monoclonal antibodies suggested that the therapeutic potential of monoclonal antibodies would be severely limited by the rapid emergence of viral escape mutations in the context of diverse virus swarms[15–17]. However, cocktails of three or five of the new generation of more potent monoclonal antibodies targeting multiple epitopes have recently been shown to suppress HIV-1 replication in humanized mice[18,19].

Therapeutic efficacy of monoclonal antibody cocktails

To evaluate the therapeutic potential of broad and potent HIV-1-specific monoclonal antibodies in primates with an intact immune system, we infused cocktails of monoclonal antibodies as well as single monoclonal antibodies into chronically SHIV-infected rhesus monkeys. We focused on the N332 glycan-dependent monoclonal antibody PGT121 (ref. 10) and the CD4-binding-site-specific monoclonal antibodies 3BNC117 (ref. 6) and b12 (ref. 20). In the first study, we used eight Indian origin adult rhesus monkeys (*Macaca mulatta*) that did not express the class I alleles *Mamu-A*01*, *Mamu-B*08* and *Mamu-B*17* and that were infected intrarectally with the pathogenic virus SHIV-SF162P3 9 months before the monoclonal antibody infusions. These animals exhibited chronic set-point viral loads of 3.4–4.9 log RNA copies ml^{-1} with clinical disease progression and reduced $CD4^+$ T-lymphocyte counts. We performed two intravenous monoclonal antibody infusions on day 0 and day 7 with 10 mg kg^{-1} of each of PGT121, 3BNC117 and b12 ($n = 4$); or with 30 mg kg^{-1} of the isotype-matched control monoclonal antibody DEN3 ($n = 1$) or saline ($n = 3$).

After the initial monoclonal antibody infusion, we observed rapid and precipitous declines of plasma viral loads to undetectable levels by day 7 in 4 of 4 monkeys (Fig. 1a). Virological control persisted for 84 to 98 days in animals 82-09, 98-09 and 161-09 (Fig. 1b). After viral rebound, sequence analysis[18,21] showed no N332 or other characteristic escape mutations (Supplementary Information), and viral rebound correlated with the decline of serum monoclonal antibody titres to undetectable levels <1 μg ml^{-1} (Extended Data Fig. 1). Monkey 82-09 exhibited transient viraemia on day 28 (Fig. 1b), which correlated with the decline of serum monoclonal antibody titres to undetectable levels (Extended Data Fig. 1), but this animal then spontaneously re-controlled viral replication until day 98. Monkey 163-09, which had the lowest baseline viral load of 3.4 log RNA copies ml^{-1} before the monoclonal antibody infusion, exhibited long-term virological control for over

[1]Center for Virology and Vaccine Research, Beth Israel Deaconess Medical Center, Harvard Medical School, Boston, Massachusetts 02215, USA. [2]Ragon Institute of MGH, MIT, and Harvard, Cambridge, Massachusetts 02139, USA. [3]The Scripps Research Institute, La Jolla, California 92037, USA. [4]The Rockefeller University, New York, New York 10065, USA. [5]Massachusetts Institute of Technology, Cambridge, Massachusetts 02139, USA. [6]New England Primate Research Center, Southborough, Massachusetts 01776, USA. [7]Bioqual, Inc., Rockville, Maryland 20852, USA. [8]Alpha Genesis, Inc., Yemassee, South Carolina 29945, USA. [9]Howard Hughes Medical Institute, New York, New York 10065, USA.
*These authors contributed equally to this work.

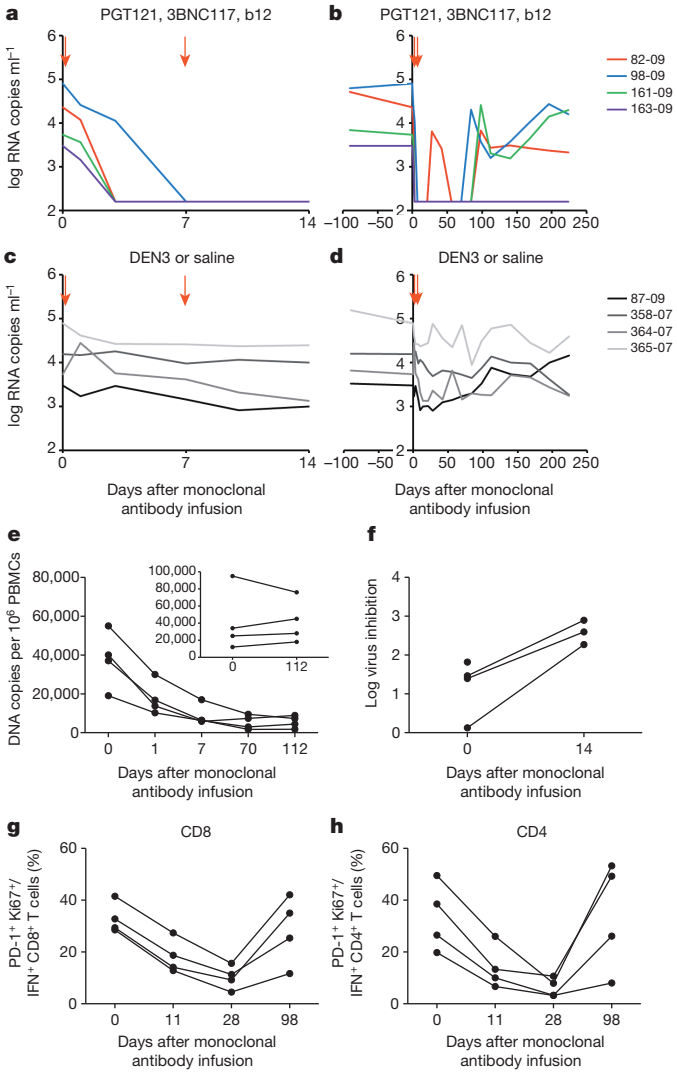

Figure 1 | Therapeutic efficacy of the triple PGT121, 3BNC117 and b12 monoclonal antibody cocktail. **a**, **b**, Plasma viral RNA (log copies ml^{-1}) in rhesus monkeys chronically infected with SHIV-SF162P3 after infusions of PGT121, 3BNC117 and b12 on day 0 and day 7 (arrows) for 14 days (**a**) and 224 days (**b**). **c**, **d**, Plasma viral RNA in rhesus monkeys chronically infected with SHIV-SF162P3 after infusions with the control monoclonal antibody DEN3 (87-09) or saline on day 0 and day 7 (arrows) for 14 days (**c**) and 224 days (**d**). **e**, Proviral DNA (copies per 10^6 peripheral blood mononuclear cells (PBMCs)) in the monkeys that received the therapeutic monoclonal antibody cocktail or controls (inset). **f**, Log inhibition of viral replication in $CD8^+$ T-lymphocyte-dependent virus suppression assays after monoclonal antibody infusion. One animal had no recoverable virus at week 2. **g**, **h**, $PD\text{-}1^+Ki67^+$ expression on Gag-specific $CD8^+$ (**g**) and $CD4^+$ (**h**) T lymphocytes after monoclonal antibody infusion.

200 days despite the absence of detectable serum monoclonal antibody titres after day 70 (Fig. 1b). Proviral DNA in peripheral blood also declined rapidly by tenfold in the monkeys that received the monoclonal antibodies (Fig. 1e). Virological control was not observed in the monkeys that received DEN3 or saline (Fig. 1c, d), and viral loads on day 14 were significantly lower in the monoclonal-antibody-treated monkeys than in the controls ($P = 0.02$, Mann–Whitney U-test).

As expected, serum neutralizing antibody titres[22] to the SHIV-SF162P3 challenge virus increased markedly after the monoclonal antibody administration and then declined over time (Extended Data Fig. 2). After clearance of the monoclonal antibodies, neutralizing antibody titres to SHIV-SF162P3 as well as to the related neutralization-sensitive virus SHIV-SF162P4 remained slightly higher than baseline titres (Extended Data Fig. 2). The magnitude of total Gag-specific $CD8^+$ and $CD4^+$ T-lymphocyte responses[23,24] was not detectably modulated after monoclonal antibody administration (Extended Data Fig. 3). However, by day 28, we observed threefold and fivefold reductions, respectively, in the percentage of Gag-specific $CD8^+$ and $CD4^+$ T lymphocytes that expressed the exhaustion and activation markers PD-1 and Ki67 (Fig. 1g, h; $P = 0.02$). Moreover, $CD8^+$ T lymphocytes from these animals exhibited increased functional capacity to suppress virus replication after monoclonal antibody infusion[25] (Fig. 1f; $P = 0.03$). These data indicate that monoclonal antibody administration not only exerted direct antiviral effects but also improved host immune responses.

We next investigated the therapeutic efficacy of a single infusion of the cocktail of three monoclonal antibodies as well as a combination of only two monoclonal antibodies. Fourteen rhesus monkeys infected with SHIV-SF162P3 9 months before the monoclonal antibody infusion with chronic set-point viral loads of 3.2–5.6 log RNA copies ml^{-1} received a single infusion on day 0 with 10 mg kg^{-1} of each of the monoclonal antibodies PGT121, 3BNC117 and b12 ($n = 5$); PGT121 and 3BNC117 ($n = 5$); or the isotype-matched control monoclonal antibody DEN3 ($n = 4$). We observed rapid virological control to undetectable levels by day 7 in 3 of 5 animals that received the cocktail of three monoclonal antibodies and in 5 of 5 animals that received only PGT121 and 3BNC117 (Fig. 2a, b). The two animals that failed to achieve complete virological suppression had the highest baseline plasma viral loads of 5.4 and 5.6 log RNA copies ml^{-1} before the monoclonal antibody infusion and exhibited 2.8 and 2.9 log declines, respectively, in plasma viraemia before rapid viral rebound on day 21 (monkeys 4907, 4909; Fig. 2a). No characteristic viral escape mutations were detected after viral rebound (Supplementary Information). The animals that suppressed viral loads to undetectable levels exhibited up to a 3.1 log decline of plasma viral RNA copies ml^{-1} by day 7 (monkey 4912; Fig. 2b). Viral rebound occurred in most animals between day 28 and day 84 (Fig. 2a, b) and was associated with declines of serum monoclonal antibody titres to undetectable levels (Extended Data Fig. 4). The animal with the lowest baseline viral load of 3.2 log RNA copies ml^{-1} exhibited long-term virological control for over 100 days (monkey 4905; Fig. 2b), and viral loads on day 14 were significantly lower in both groups of monoclonal-antibody-treated monkeys than in the controls ($P = 0.01$). One control animal (monkey 5324; Fig. 2c) was euthanized for progressive clinical AIDS and opportunistic infections during the course of this experiment. PGT121 and 3BNC117 administration also resulted in threefold and fourfold reductions in the percentage of $PD\text{-}1^+Ki67^+$ Gag-specific $CD8^+$ and $CD4^+$ T lymphocytes, respectively (Fig. 2e, f).

To confirm that viral rebound was not associated with the development of viral resistance to the monoclonal antibodies, we performed a second infusion of monoclonal antibodies on day 105 in the monkeys that received PGT121 and 3BNC117. Viral re-suppression was observed in 4 of 4 animals after the second monoclonal antibody infusion (Fig. 2d and Supplementary Information). However, virological control appeared less durable and serum monoclonal antibody titres were lower after the second monoclonal antibody infusion as compared with the first monoclonal antibody infusion (Fig. 2b, d and Extended Data Fig. 4), presumably as a result of monkey anti-human antibody responses that developed after the first monoclonal antibody administration (Extended Data Fig. 5). Nevertheless, we assessed the impact of the second monoclonal antibody infusion on proviral DNA in various tissue compartments[26,27] and observed a twofold decline in lymph nodes ($P = 0.1$; Fig. 2g) and a threefold decline in gastrointestinal mucosa ($P = 0.02$; Fig. 2h) 14 days after monoclonal antibody re-administration. These data indicate that the potent monoclonal antibodies not only suppressed viraemia but also reduced proviral DNA in tissues without the generation of viral resistance.

Therapeutic efficacy of single monoclonal antibodies

Although the cloned SHIV-SF162P3 pseudovirus is highly sensitive to 3BNC117, we observed that our particular SHIV-SF162P3 challenge

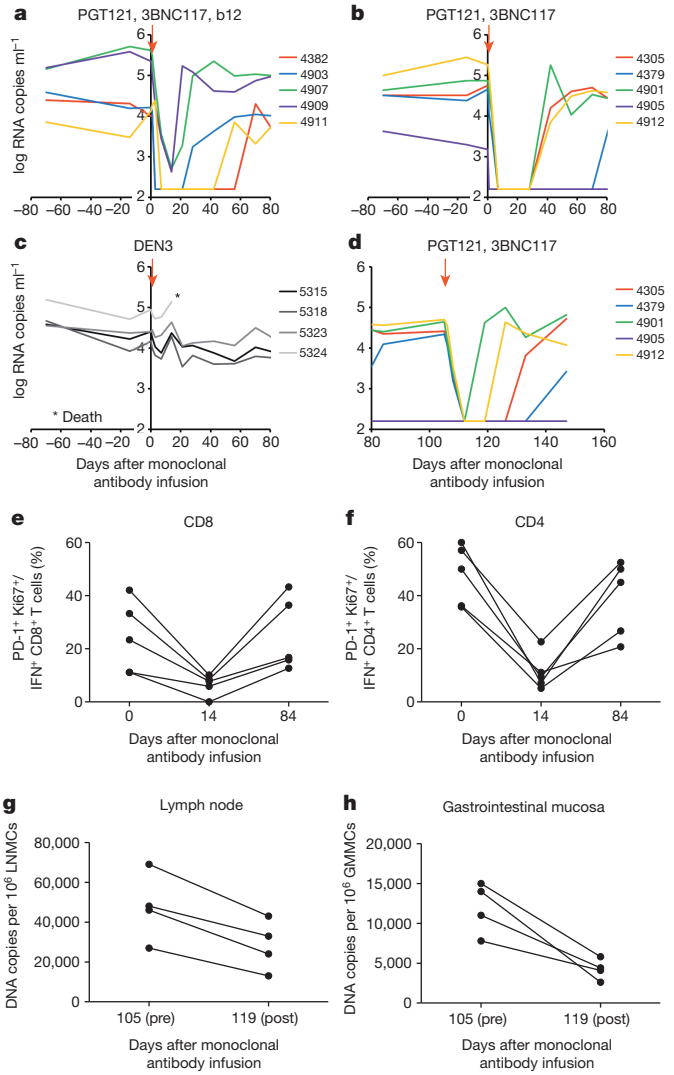

Figure 2 | Therapeutic efficacy of the double PGT121 and 3BNC117 monoclonal antibody cocktail. **a**–**c**, Plasma viral RNA (log copies ml^{-1}) in rhesus monkeys chronically infected with SHIV-SF162P3 after a single infusion (arrows) of PGT121, 3BNC117 and b12 (**a**); PGT121 and 3BNC117 (**b**); or the control monoclonal antibody DEN3 (**c**). **d**, Plasma viral RNA in monkeys after a second infusion of PGT121 and 3BNC117 on day 105. **e**, **f**, PD-1^+Ki67^+ expression on Gag-specific $CD8^+$ (**e**) and $CD4^+$ (**f**) T lymphocytes in the monkeys that received PGT121 and 3BNC117. **g**, **h**, Proviral DNA (copies per 10^6 cells) in lymph nodes (**g**) and gastrointestinal mucosa (**h**) before (day 105) and 14 days after (day 119) the second monoclonal antibody infusion with PGT121 and 3BNC117 in the four animals with detectable viraemia. GMMCs, gastrointestinal mucosa mononuclear cells; LNMCs, lymph node mononuclear cells.

stock was largely resistant to 3BNC117 (Extended Data Fig. 6), which raised the possibility that the observed therapeutic efficacy of the monoclonal antibody cocktail in the previous experiment may have been due to PGT121 alone. We therefore performed a single infusion of 10 mg kg^{-1} PGT121 alone ($n = 4$), 3BNC117 alone ($n = 4$), or the control monoclonal antibody DEN3 ($n = 4$) in 12 rhesus monkeys that were infected with SHIV-SF162P3 9 months before the monoclonal antibody infusion with chronic set-point viral loads of 3.3–5.4 log RNA copies ml^{-1}. PGT121 alone resulted in rapid virological control to undetectable levels by day 7 in 4 of 4 animals, followed by viral rebound by day 42 to day 56 in 3 animals that again correlated with declines in serum PGT121 titres to undetectable levels (Fig. 3a, c and Extended Data Fig. 7; $P = 0.02$ comparing viral loads on day 14 in PGT121-treated animals compared with controls). One animal exhibited long-term virological control (monkey DN1G; Fig. 3a). PGT121 alone also reduced proviral DNA by sixfold in peripheral blood ($P = 0.05$; Fig. 3d), fourfold in lymph nodes ($P = 0.05$; Fig. 3e), and fourfold in gastrointestinal mucosa ($P = 0.1$; Fig. 3f) as compared with the DEN3 control on day 14. Moreover, PGT121 alone resulted in threefold and fivefold reductions in the percentage of PD-1^+Ki67^+ Gag-specific $CD8^+$ and $CD4^+$ T lymphocytes, respectively (Fig. 3g, h). In contrast, 3BNC117 alone, to which our SHIV-SF162P3 stock was relatively resistant, resulted in only a transient 0.2–1.1 log reduction of plasma viral loads (Fig. 3b), and one animal in this group (monkey CW9G) was euthanized for progressive clinical AIDS during this experiment.

Kinetics of virological control

The kinetics of the initial decline of plasma viraemia after infusion of PGT121 or PGT121-containing monoclonal antibody cocktails was a median of 0.382 logs per day (inter-quartile range (IQR) 0.338–0.540). In contrast, the initial kinetics of decline of plasma viraemia after raltegravir-containing combination antiretroviral therapy in HIV-1-infected humans was a median of 0.264 logs per day (IQR 0.253–0.284)[28]

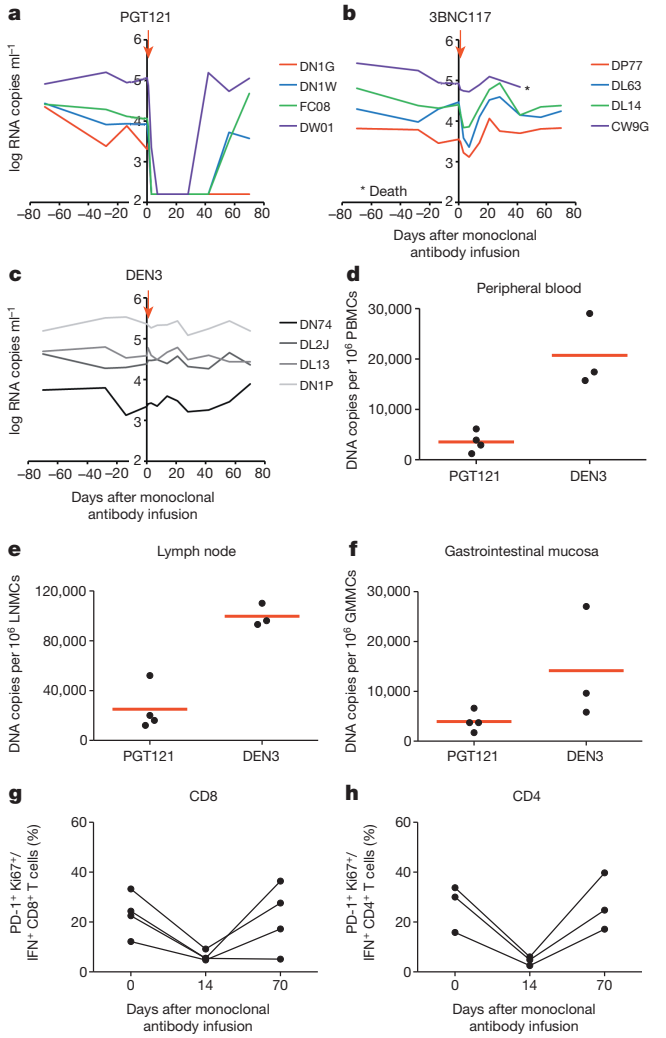

Figure 3 | Therapeutic efficacy of the single monoclonal antibodies PGT121 and 3BNC117. **a**–**c**, Plasma viral RNA (log copies ml^{-1}) in rhesus monkeys chronically infected with SHIV-SF162P3 after a single infusion (arrows) of PGT121 (**a**), 3BNC117 (**b**), or the control monoclonal antibody DEN3 (**c**). **d**–**f**, Proviral DNA (copies per 10^6 cells) in peripheral blood mononuclear cells (PBMCs) (**d**), lymph nodes (**e**) and gastrointestinal mucosa (**f**) 14 days after the monoclonal antibody infusion in the animals that received PGT121 or DEN3. Red bars indicate mean values. Assays for one of the DEN3-treated controls failed. **g**, **h**, PD-1^+Ki67^+ expression on Gag-specific $CD8^+$ (**g**) and $CD4^+$ (**h**) T lymphocytes in the monkeys that received PGT121.

and after combination antiretroviral therapy in SIV-infected monkeys was a median of 0.229 logs per day (IQR 0.198–0.265) (J.B.W., unpublished data) (Extended Data Table 1). Although these reflect different models, the rapid virological control after monoclonal antibody administration in SHIV-infected rhesus monkeys is striking and consistent with a mechanism that involves direct elimination of free virus in plasma in addition to virus-infected cells in tissues. The rapid reduction of proviral DNA in peripheral blood by day 1 (Fig. 1e) suggests direct antibody-mediated cytotoxic effects on infected cells[29], although we cannot exclude the possibility of an effect of $CD4^+$ T-cell trafficking.

Summary and implications

Our studies demonstrate the profound therapeutic efficacy of PGT121 and PGT121-containing monoclonal antibody cocktails in chronically SHIV-SF162P3 infected rhesus monkeys. The therapeutic efficacy in the 18 animals that received PGT121 alone or as part of a cocktail (Fig. 4a) was dependent on baseline viral loads before monoclonal antibody administration. In the 17% of animals (3 of 18) with low baseline viral loads <3.5 log RNA copies ml^{-1}, long-term control of viral replication was observed for the duration of the follow-up period (Fig. 4b), which included a substantial period of time after serum monoclonal antibody titres had declined to undetectable levels. These observations suggest that PGT121 may have converted animals with low baseline viraemia into 'elite controllers', although additional follow-up is required to assess the durability of this effect. These animals still had detectable, albeit reduced, proviral DNA in tissues (Figs 2g, h and 3e, f), and thus virus was not eradicated in these animals. In the 72% of animals (13 of 18) with intermediate baseline viral loads 3.5–5.3 log RNA copies ml^{-1}, plasma viraemia was rapidly reduced to undetectable levels within 7 days but then rebounded after a median of 56 days when serum monoclonal antibody titres declined to undetectable levels <1 μg ml^{-1} (Fig. 4c). In the 11% of animals (2 of 18) with high baseline viral loads >5.3 log RNA copies ml^{-1}, incomplete control of plasma viraemia and rapid viral rebound was observed, indicating a therapeutic ceiling in this model (Fig. 4d). Taken together, baseline viral loads strongly correlated with the time to viral rebound ($P = 0.0002$, Spearman rank-correlation test; Fig. 4e).

We speculate that the therapeutic impact of these monoclonal antibodies reflected not only their direct antiviral activity but also their impact on host antiviral immune responses. After monoclonal antibody infusion, we observed modest increases in host virus-specific neutralizing antibody activity (Extended Data Fig. 2) as well as reduced activation and improved functionality of host virus-specific T-lymphocyte responses (Figs 1f–h, 2e, f and 3g, h). Consistent with these findings, median set-point viral loads after viral rebound were 0.61 log lower than median set-point viral loads at baseline before monoclonal antibody infusion ($P = 0.0005$, Wilcoxon matched pairs signed-rank test; Fig. 4f), with no evidence of reduced viral replicative capacity[30] (Extended Data Fig. 8). Moreover, 3 of 18 monkeys exhibited long-term virological control to undetectable levels (Fig. 4b). Defining the precise immunological mechanisms of improved virological control after monoclonal and polyclonal antibody administration[31,32] warrants further investigation.

Previous studies in humanized mice and humans showed that the earlier generation of neutralizing HIV-1-specific monoclonal antibodies was unable to control viraemia[15–17]. More recent studies in humanized mice have shown that combinations of three or five of the new generation of more potent monoclonal antibodies suppressed HIV-1 replication, although single monoclonal antibodies still rapidly selected for resistance[18,19]. In contrast to these previous studies, we observed that a single infusion of PGT121 in rhesus monkeys resulted in rapid virological control in both peripheral blood and tissues. It is possible that intrinsic differences between HIV-1 replication in mice and SHIV replication in monkeys may account for these differences. Another key difference is the functional immune system in rhesus monkeys as compared with immunosuppressed humanized mice, and the profound virological suppression without the development of

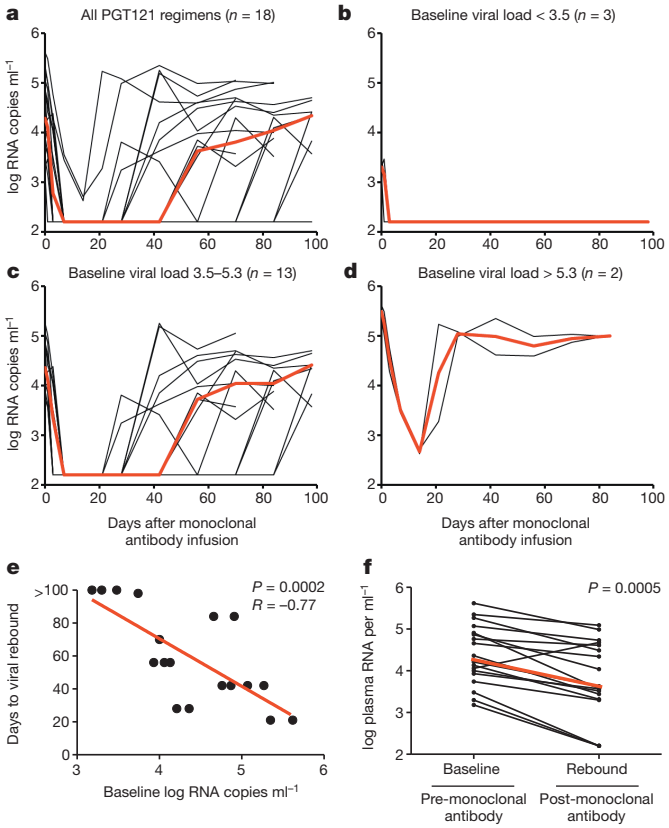

Figure 4 | Therapeutic efficacy of PGT121 or PGT121-containing monoclonal antibody cocktails in chronically SHIV-infected rhesus monkeys. a–d, Summary of the therapeutic effect of PGT121 alone or PGT121-containing monoclonal antibody cocktails in the 18 rhesus monkeys chronically infected with SHIV-SF162P3 (**a**), as well as in the subgroups of animals with baseline viral loads of <3.5 log RNA copies ml^{-1} ($n = 3$) (**b**), 3.5–5.3 log RNA copies ml^{-1} ($n = 13$) (**c**) and >5.3 log RNA copies ml^{-1} ($n = 2$) (**d**). Red lines indicate median log viral loads. **e**, Correlation of baseline viral loads with times to viral rebound. *P* value reflects two-sided Spearman rank-correlation test. **f**, Comparison of set-point viral loads at baseline before monoclonal antibody administration and after viral rebound. *P* value reflects two-sided Wilcoxon matched pairs signed-rank test. Red line indicates median log viral loads.

resistance in the present study may reflect the functional host antibody effector activity and the intact antiviral cellular immune responses in rhesus monkeys. A caveat is that we were unable to quantify the intrinsic ability of SHIV-SF162P3 to escape from PGT121 *in vivo*, although previous studies have documented the ability of SHIV-SF162P3 and SHIV-SF162P4 to escape from autologous antibody responses in other settings[33,34]. N332A-mutated SHIV-SF162P3 exhibited only partial escape from PGT121 *in vitro* but complete escape from other N332-dependent monoclonal antibodies including PGT124 and PGT128, suggesting a high bar to resistance (Extended Data Fig. 9).

Concluding remarks

Our data demonstrate profound therapeutic efficacy of broad and potent HIV-1-specific monoclonal antibodies in rhesus monkeys chronically infected with SHIV-SF162P3. Our SHIV-SF162P3 stock is highly pathogenic, as evidenced by moderate to high chronic set-point viral loads and AIDS-related deaths in two animals during the course of these experiments (Figs 2c and 3b). Moreover, in a separate study[35], our SHIV-SF162P3 stock led to AIDS-related mortality in 5 of 12 (42%) rhesus monkeys by 1 year after infection, which is comparable to the reported pathogenicity of SIVmac251 (refs 36, 37) and greater than the reported mortality of SHIV-AD8 (refs 38, 39). Nevertheless, given the differences between SHIV-infected rhesus

monkeys and HIV-1-infected humans, clinical trials will be required to establish the therapeutic efficacy of potent neutralizing HIV-1-specific monoclonal antibodies in humans. Although multiple monoclonal antibodies targeting different epitopes will probably prove to be superior, our data suggest that monotherapy with the most potent and broad monoclonal antibodies also warrants clinical evaluation. Moreover, the ability of these monoclonal antibodies to reduce proviral DNA in tissues suggests that these monoclonal antibodies should also be evaluated in the context of viral eradication strategies.

METHODS SUMMARY

Thirty-four Indian origin, young adult, male and female rhesus monkeys (*Macaca mulatta*) that were infected by the intrarectal route with SHIV-SF162P3 and followed 9 months before monoclonal antibody administration were used for these studies. Cocktails of monoclonal antibodies (PGT121, 3BNC117, b12) or single monoclonal antibodies (PGT121, 3BNC117) were administered once or twice at 10 mg kg^{-1} for each monoclonal antibody by the intravenous route. DEN3 was used as an isotype-matched monoclonal antibody control. Monkeys were bled up to three times per week for evaluation of plasma viral loads. Lymph node and gastrointestinal mucosal biopsies were processed as single cell suspensions[27] for proviral DNA assays as previously described[26]. SIV Gag-specific cellular immune responses were assessed by multiparameter intracellular cytokine staining (ICS) assays[23,24] and functional virus suppression assays[25] essentially as described. HIV-1-specific neutralizing antibody responses were assessed by TZM-bl luciferase-based neutralization assays[22]. PGT121, 3BNC117 and b12 concentrations were determined by monoclonal-antibody-specific neutralizing antibody assays. Virus sequencing and analyses of breakthrough viruses were performed essentially as described[18,21]. Statistical analyses involved Mann–Whitney *U*-tests for comparing independent sets of virological and immunologic parameters, Wilcoxon matched pairs signed-rank tests for paired analyses, and Spearman rank-correlation tests for correlation analyses.

Online Content Any additional Methods, Extended Data display items and Source Data are available in the online version of the paper; references unique to these sections appear only in the online paper.

Received 22 July; accepted 8 October 2013.
Published online 30 October 2013.

1. Burton, D. R., Poignard, P., Stanfield, R. L. & Wilson, I. A. Broadly neutralizing antibodies present new prospects to counter highly antigenically diverse viruses. *Science* **337,** 183–186 (2012).
2. Klein, F. *et al.* Antibodies in HIV-1 vaccine development and therapy. *Science* **341,** 1199–1204 (2013).
3. Wu, X. *et al.* Rational design of envelope identifies broadly neutralizing human monoclonal antibodies to HIV-1. *Science* **329,** 856–861 (2010).
4. Zhou, T. *et al.* Structural basis for broad and potent neutralization of HIV-1 by antibody VRC01. *Science* **329,** 811–817 (2010).
5. Scheid, J. F. *et al.* Broad diversity of neutralizing antibodies isolated from memory B cells in HIV-infected individuals. *Nature* **458,** 636–640 (2009).
6. Scheid, J. F. *et al.* Sequence and structural convergence of broad and potent HIV antibodies that mimic CD4 binding. *Science* **333,** 1633–1637 (2011).
7. Diskin, R. *et al.* Increasing the potency and breadth of an HIV antibody by using structure-based rational design. *Science* **334,** 1289–1293 (2011).
8. Walker, L. M. *et al.* Broad and potent neutralizing antibodies from an African donor reveal a new HIV-1 vaccine target. *Science* **326,** 285–289 (2009).
9. McLellan, J. S. *et al.* Structure of HIV-1 gp120 V1/V2 domain with broadly neutralizing antibody PG9. *Nature* **480,** 336–343 (2011).
10. Walker, L. M. *et al.* Broad neutralization coverage of HIV by multiple highly potent antibodies. *Nature* **477,** 466–470 (2011).
11. Julien, J. P. *et al.* Broadly neutralizing antibody PGT121 allosterically modulates CD4 binding via recognition of the HIV-1 gp120 V3 base and multiple surrounding glycans. *PLoS Pathog.* **9,** e1003342 (2013).
12. Mouquet, H. *et al.* Complex-type N-glycan recognition by potent broadly neutralizing HIV antibodies. *Proc. Natl Acad. Sci. USA* **109,** E3268–E3277 (2012).
13. Kong, L. *et al.* Supersite of immune vulnerability on the glycosylated face of HIV-1 envelope glycoprotein gp120. *Nature Struct. Mol. Biol.* **20,** 796–803 (2013).
14. Huang, J. *et al.* Broad and potent neutralization of HIV-1 by a gp41-specific human antibody. *Nature* **491,** 406–412 (2012).
15. Poignard, P. *et al.* Neutralizing antibodies have limited effects on the control of established HIV-1 infection *in vivo*. *Immunity* **10,** 431–438 (1999).
16. Trkola, A. *et al.* Delay of HIV-1 rebound after cessation of antiretroviral therapy through passive transfer of human neutralizing antibodies. *Nature Med.* **11,** 615–622 (2005).
17. Mehandru, S. *et al.* Adjunctive passive immunotherapy in human immunodeficiency virus type 1-infected individuals treated with antiviral therapy during acute and early infection. *J. Virol.* **81,** 11016–11031 (2007).
18. Klein, F. *et al.* HIV therapy by a combination of broadly neutralizing antibodies in humanized mice. *Nature* **492,** 118–122 (2012).
19. Diskin, R. *et al.* Restricting HIV-1 pathways for escape using rationally designed anti-HIV-1 antibodies. *J. Exp. Med.* **210,** 1235–1249 (2013).
20. Burton, D. R. *et al.* Efficient neutralization of primary isolates of HIV-1 by a recombinant human monoclonal antibody. *Science* **266,** 1024–1027 (1994).
21. West, A. P. Jr *et al.* Computational analysis of anti-HIV-1 antibody neutralization panel data to identify potential functional epitope residues. *Proc. Natl Acad. Sci. USA* **110,** 10598–10603 (2013).
22. Montefiori, D. *Evaluating Neutralizing Antibodies Against HIV, SIV and SHIV in Luciferase Reporter Gene Assays. Current Protocols Immunol* (John Wiley & Sons, 2004).
23. Pitcher, C. J. *et al.* Development and homeostasis of T cell memory in rhesus macaque. *J. Immunol.* **168,** 29–43 (2002).
24. Liu, J. *et al.* Magnitude and phenotype of cellular immune responses elicited by recombinant adenovirus vectors and heterologous prime-boost regimens in rhesus monkeys. *J. Virol.* **82,** 4844–4852 (2008).
25. Stephenson, K. E., Li, H., Walker, B. D., Michael, N. L. & Barouch, D. H. Gag-specific cellular immunity determines *in vitro* viral inhibition and *in vivo* virologic control following simian immunodeficiency virus challenges of vaccinated rhesus monkeys. *J. Virol.* **86,** 9583–9589 (2012).
26. Whitney, J. B. *et al.* T-cell vaccination reduces simian immunodeficiency virus levels in semen. *J. Virol.* **83,** 10840–10843 (2009).
27. Li, H. *et al.* Durable mucosal simian immunodeficiency virus-specific effector memory T lymphocyte responses elicited by recombinant adenovirus vectors in rhesus monkeys. *J. Virol.* **85,** 11007–11015 (2011).
28. Andrade, A. *et al.* Three distinct phases of HIV-1 RNA decay in treatment-naive patients receiving raltegravir-based antiretroviral therapy: ACTG A5248. *J. Infect. Dis.* **208,** 884–891 (2013).
29. Horwitz, J. A. *et al.* HIV-1 suppression and durable control by combining single broadly neutralizing antibodies and antiretroviral drugs in humanized mice. *Proc. Natl Acad. Sci. USA* **110,** 16538–16543 (2013).
30. Cornall, A. *et al.* A novel, rapid method to detect infectious HIV-1 from plasma of persons infected with HIV-1. *J. Virol. Methods* **165,** 90–96 (2010).
31. Jaworski, J. P. *et al.* Neutralizing polyclonal IgG present during acute infection prevents rapid disease onset in simian-human immunodeficiency virus SHIVSF162P3-infected infant rhesus macaques. *J. Virol.* **87,** 10447–10459 (2013).
32. Ng, C. T. *et al.* Passive neutralizing antibody controls SHIV viremia and enhances B cell responses in infant macaques. *Nature Med.* **16,** 1117–1119 (2010).
33. Jayaraman, P. *et al.* Evidence for persistent, occult infection in neonatal macaques following perinatal transmission of simian-human immunodeficiency virus SF162P3. *J. Virol.* **81,** 822–834 (2007).
34. Kraft, Z. *et al.* Macaques infected with a CCR5-tropic simian/human immunodeficiency virus (SHIV) develop broadly reactive anti-HIV neutralizing antibodies. *J. Virol.* **81,** 6402–6411 (2007).
35. Barouch, D. H. *et al.* Protective efficacy of a global HIV-1 mosaic vaccine against heterologous SHIV challenges in rhesus monkeys. *Cell* **155,** 531–539 (2013).
36. Barouch, D. H. *et al.* Vaccine protection against acquisition of neutralization-resistant SIV challenges in rhesus monkeys. *Nature* **482,** 89–93 (2012).
37. Liu, J. *et al.* Immune control of an SIV challenge by a T-cell-based vaccine in rhesus monkeys. *Nature* **457,** 87–91 (2009).
38. Nishimura, Y. *et al.* Generation of the pathogenic R5-tropic simian/human immunodeficiency virus SHIVAD8 by serial passaging in rhesus macaques. *J. Virol.* **84,** 4769–4781 (2010).
39. Gautam, R. *et al.* Pathogenicity and mucosal transmissibility of the R5-tropic simian/human immunodeficiency virus SHIV(AD8) in rhesus macaques: implications for use in vaccine studies. *J. Virol.* **86,** 8516–8526 (2012).

Supplementary Information is available in the online version of the paper.

Acknowledgements We thank A. Brinkman, M. Ferguson, C. Gittens, R. Geleziunas, R. Hamel, K. Kelly, J. Kramer, A. McNally, D. Montefiori, L. Nogueira, L. Parenteau, M. Pensiero, L. Peter, M. Shetty, D. Sok, K. Stanley, F. Stephens, W. Wagner, B. Walker, A. West and J. Yalley-Ogunro for advice, assistance and reagents. The SIVmac239 Gag peptide pool was obtained from the NIH AIDS Research and Reference Reagent Program. We acknowledge support from the National Institutes of Health (AI055332, AI060354, AI078526, AI084794, AI095985, AI096040, AI10063, AI100148, AI100663); the Bill and Melinda Gates Foundation (OPP1033091, OPP1033115, OPP1040741, OPP1040753); the Ragon Institute of MGH, MIT, and Harvard; the Lundbeck Foundation; and the Stavros Niarchos Foundation. M.C.N. is a Howard Hughes Medical Institute investigator. M.C.N. and D.R.B. are co-inventors on patents covering the monoclonal antibodies used in the present study.

Author Contributions D.H.B., M.C.N. and D.R.B. designed the studies. J.B.W., B.M., F.K., T.Y.O., H.-W.C., S.S. and P.P. led the virological assays. B.M., J.L., K.E.S., M.S.S., K.M.S., E.N.B., C.C., J.Y.S., S.B. and J.R.P. led the immunological assays. K.S., S.G. and A.K.C. led the kinetic analyses. J.B.W., J.P.N., M.B., M.G.L. and W.R. led the monoclonal antibody infusions and clinical care of the rhesus monkeys. D.H.B. led the studies and wrote the paper with all co-authors.

Author Information Reprints and permissions information is available at www.nature.com/reprints. The authors declare no competing financial interests. Readers are welcome to comment on the online version of the paper. Correspondence and requests for materials should be addressed to D.H.B. (dbarouch@bidmc.harvard.edu).

METHODS

Animals and study design. Thirty-four Indian-origin, outbred, young adult, male and female, specific pathogen-free rhesus monkeys (*Macaca mulatta*) that did not express the class I alleles *Mamu-A*01*, *Mamu-B*08* and *Mamu-B*17* associated with spontaneous virological control were housed at New England Primate Research Center, Bioqual, or Alpha Genesis. Groups were balanced for susceptible and resistant TRIM5α alleles. Groups of 4–5 monkeys provided statistical power to detect large differences in viral loads, and animals were randomly allocated to balance baseline viral loads. Animals were infected by the intrarectal route with our rhesus-derived SHIV-SF162P3 challenge stock 9 months before monoclonal antibody administration. PGT121, b12 and DEN3 monoclonal antibodies were generated as previously described[10] and were expressed in Chinese hamster ovary (CHO-K1) cells and purified by protein A affinity chromatography. 3BNC117 was manufactured by Celldex Therapeutics in CHO cells and purified by chromatography and sterile filtration. All the monoclonal antibody preparations were endotoxin free. Cocktails of monoclonal antibodies or single monoclonal antibodies were administered to monkeys once or twice by the intravenous route at a dose of 10 mg kg^{-1} for each monoclonal antibody. Monkeys were bled up to three times per week for viral loads. Immunological and virological data were generated blinded. All animal studies were approved by the appropriate Institutional Animal Care and Use Committee (IACUC).

Cellular immune assays. SIV Gag-specific cellular immune responses were assessed by multiparameter intracellular cytokine staining (ICS) assays essentially as described[23,24]. 12-colour ICS assays were performed with the Aqua green-fluorescent reactive dye (Invitrogen, L23101) and predetermined titres of monoclonal antibodies (Becton Dickinson) against CD3 (SP34; Alexa Fluor 700), CD4 (OKT4; BV711, Biolegend), CD8 (SK1; allophycocyanin-cyanine 7 (APC-Cy7)), CD28 (L293; BV610), CD95 (DX2; allophycocyanin), CD69 (TP1.55.3; phycoerythrin-Texas red (energy-coupled dye; ECD); Beckman Coulter), gamma interferon (IFN-γ) (B27; phycoerythrin-cyanine 7 (PE-Cy7)), Ki67 (B56; fluorescein isothiocyanate (FITC)), CCR5 (3A9; phycoerythrin), CCR7 (3D12; Pacific Blue) and PD-1 (EH21.1; peridinin chlorophyll-A-cyanine 5.5 (PerCP-Cy5.5)). IFN-γ backgrounds were consistently $<0.01\%$ in PBMCs and LNMCs and $<0.05\%$ in colorectal biopsy specimens. Virus suppression assays were performed by co-culturing purified $CD8^+$ T lymphocytes with CD8-depleted PBMCs and monitoring p27 levels for 7–14 days essentially as described[25].

Neutralizing antibody assays. HIV-1-specific neutralizing antibody responses against primary infectious stocks of SHIV-SF162P3 and SHIV-SF162P4 were assessed by TZM-bl luciferase-based neutralization assays[22]. PGT121 titres were determined by X2088_c9 and ZM247v1(Rev-) pseudovirus neutralization, 3BNC117 titres were determined by 6041.v3.c23 and Q461.ez pseudovirus neutralization, and b12 titres were determined by Du422.1.N332A pseudovirus neutralization and B2.1 ELISA.

Proviral DNA assay. Proviral DNA was quantified as previously reported[26]. Lymph node and gastrointestinal mucosal biopsies were processed as single cell suspensions essentially as previously described[27]. Tissue-specific total cellular DNA was isolated from 5×10^6 cells using a QIAamp DNA Blood Mini kit (Qiagen). The absolute quantification of viral DNA in each sample was determined by qPCR using primers specific to a conserved region SIVmac239. All samples were directly compared to a linear virus standard and the simultaneous amplification of a fragment of human *GAPDH* gene. The sensitivity of linear standards was compared against the 3D8 cell line as a reference standard as described[26]. All PCR assays were performed with 100 and 200 ng of sample DNA.

Virus sequencing. Virus sequencing of breakthrough virus was performed essentially as described[18]. Plasma samples of 1 ml were centrifuged for 30 min at 20,000*g* and the lowest fraction was subjected to RNA purification (QiaAmp MinElute Virus Spin kit; Qiagen). Random hexamers (Roche) or SHIV-SF162P3-specific (5′-AAGAGCTCCTCCAGACAGTGAG-3′ or 5′-TAGAGCCCTGGA AGCATCCAGGAAGTCAGCCTA-3′) primers were used for cDNA synthesis with SuperScript III Reverse Transcriptase (Invitrogen). SHIV envelope sequences were amplified by a double–nested PCR approach using the Expand High Fidelity PCR System (Roche). First round primers for gp120 were 5′-AAGAGCTCC TCCAGACAGTGAG-3′ and 5′-ATGAGTTTTCCAGAGCAACCC-3′ and for gp160 were 5′-AAGAGCTCCTCCAGACAGTGAG-3′ and 5′-CAAGCCCTTGT CTAATCCTCC-3′. Second round primers for gp120 were 5′-GAAAGAGCAGA AGACAGTGGC-3′ and 5′-ATTGTCTGGCCTGTACCGTC-3′ and for gp160 were 5′-GAAAGAGCAGAAGACAGTGGC-3′ and 5′-ATGGAAATAGCTCCA CCCATC-3′. After second round PCR, all products were spiked with 0.5 µl Taq polymerase and incubated for 15 min at 72 °C. Amplicons were excised from a gel and purified after cloning into the pCR4-TOPO vector (Invitrogen) and expansion in One Shot TOP10 cells at 30 °C. Single colonies were sequenced using M13F/M13R primers as well as primers annealing to the envelope sequence. A consensus sequence of each clone was derived using Geneious Pro software (Biomatters), and sequence analysis was performed using Geneious Pro and antibody database software[21].

Statistical analyses. Analyses of independent virological and immunological data were performed by two-tailed Mann–Whitney *U*-tests. Analyses of paired data sets were performed by two-tailed Wilcoxon matched pairs signed-rank tests. Correlations were evaluated by Spearman rank-correlation tests. *P* values less than 0.05 were considered significant. Statistical analyses were performed using GraphPad Prism. Exponential decay rates of plasma viral loads were calculated using standard ordinary least squares regression on $\log_{10}$ (viral load) measurements versus time (days).

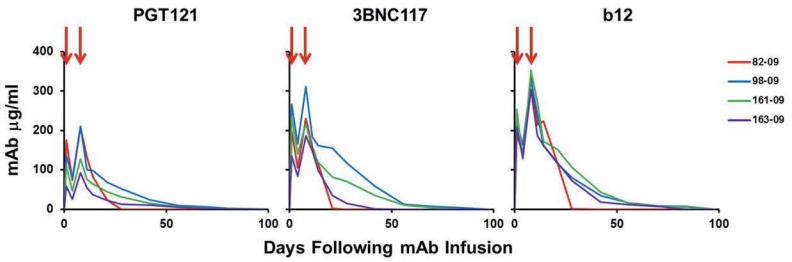

Extended Data Figure 1 | Monoclonal antibody titres after administration of the triple PGT121, 3BNC117 and b12 monoclonal antibody cocktail. PGT121, 3BNC117 and b12 titres in the monkeys described in Fig. 1 after infusion of the triple monoclonal antibody cocktail (arrows).

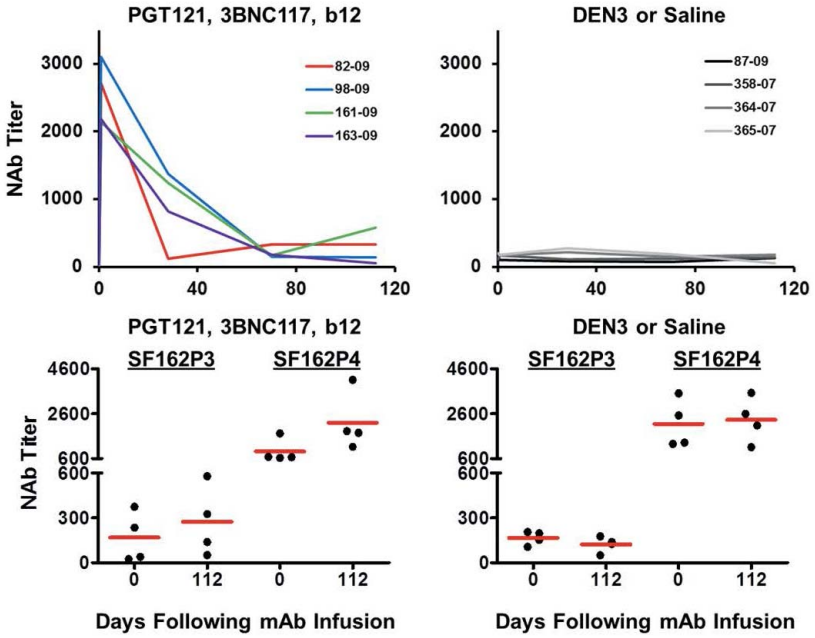

Extended Data Figure 2 | Neutralizing antibody titres after administration of the triple PGT121, 3BNC117 and b12 monoclonal antibody cocktail. SHIV-SF162P3 and SHIV-SF162P4 serum neutralizing antibody ID_{50} titres in the monkeys described in Fig. 1 after infusion of the triple monoclonal antibody cocktail (left) or saline or DEN3 (right).

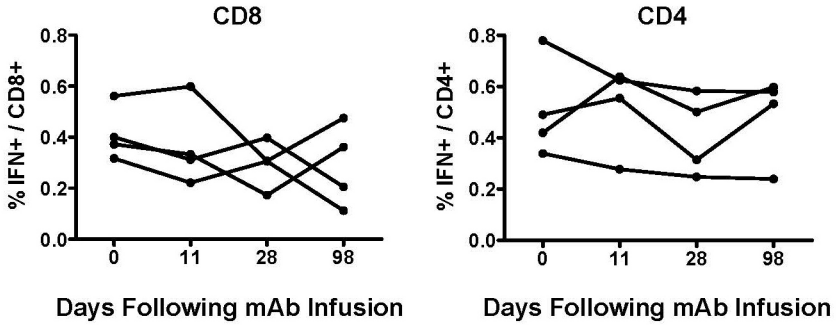

Extended Data Figure 3 | Gag-specific T lymphocyte responses after administration of the triple PGT121, 3BNC117 and b12 monoclonal antibody cocktail. Gag-specific IFN-γ^+ $CD8^+$ (left) and $CD4^+$ (right) T-lymphocyte responses by multiparameter intracellular cytokine staining assays in the monkeys described in Fig. 1 after infusion of the triple monoclonal antibody cocktail.

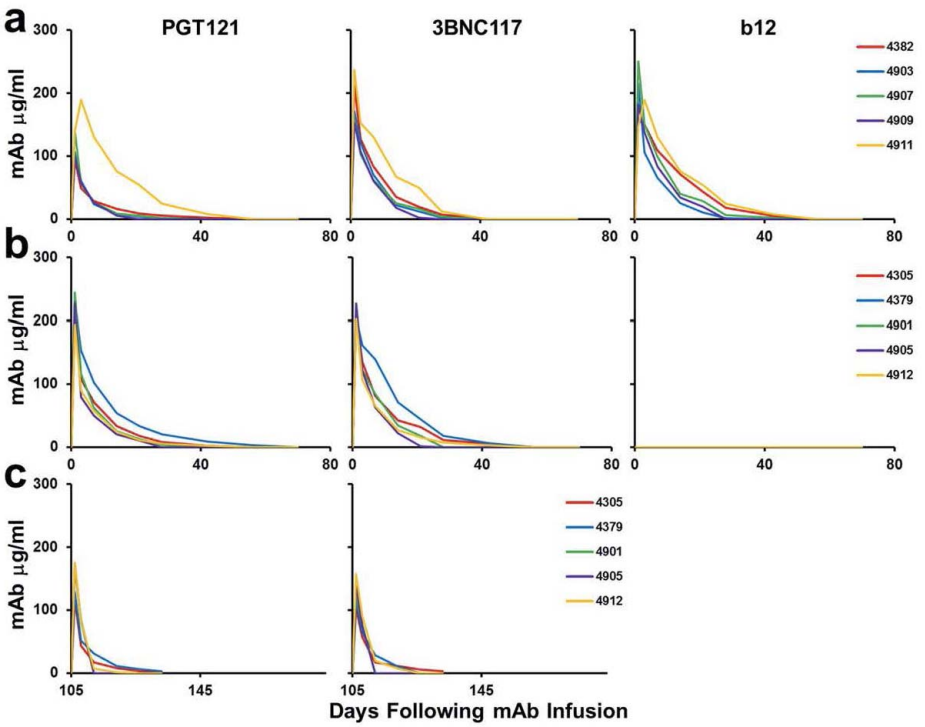

Extended Data Figure 4 | Monoclonal antibody titres after administration of the double PGT121 and 3BNC117 monoclonal antibody cocktail. **a–c**, PGT121, 3BNC117 and b12 titres in the monkeys described in Fig. 2 that received PGT121, 3BCN117 and b12 (**a**); PGT121 and 3BNC117 (**b**); or the second infusion of PGT121 and 3BNC117 (**c**).

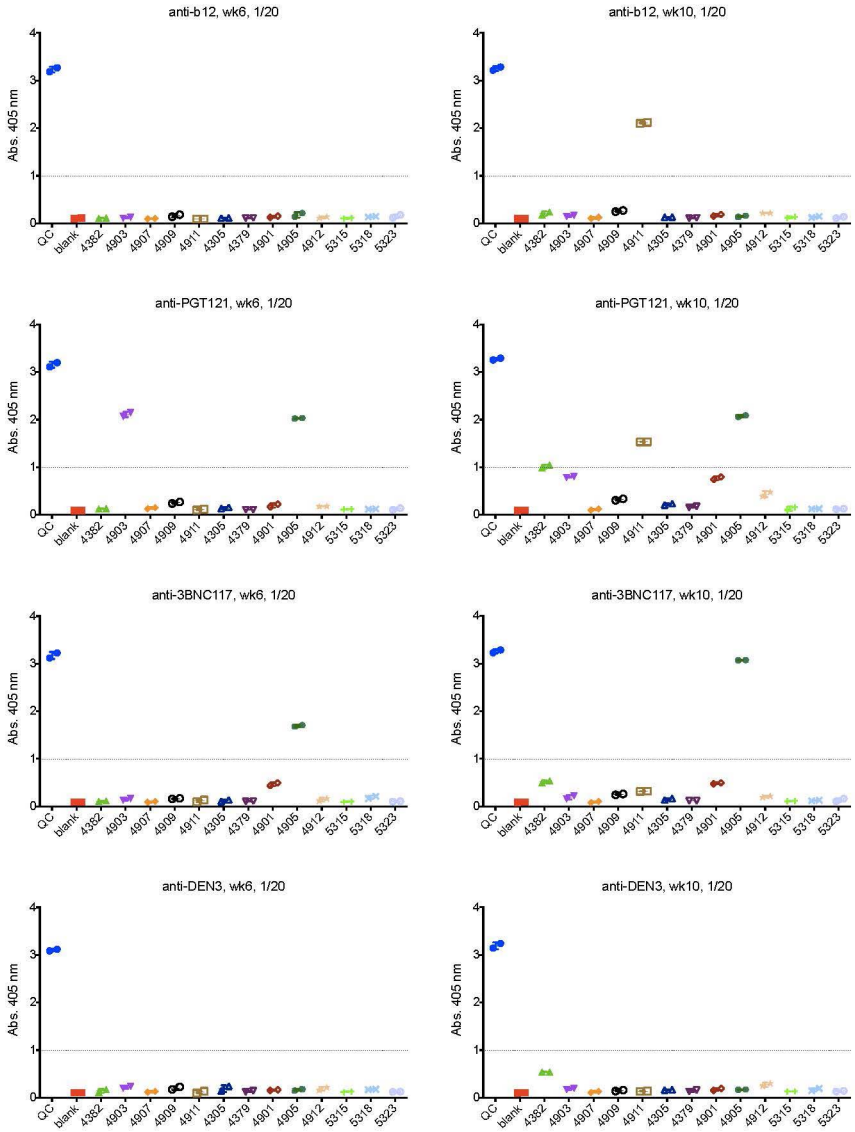

Extended Data Figure 5 | Monkey anti-human antibody titres after monoclonal antibody administration. ELISAs assessing anti-b12, anti-PGT121, anti-3BNC117 and anti-DEN3 antibodies at week 6 and week 10 after monoclonal antibody infusion in the monkeys described in Fig. 2.

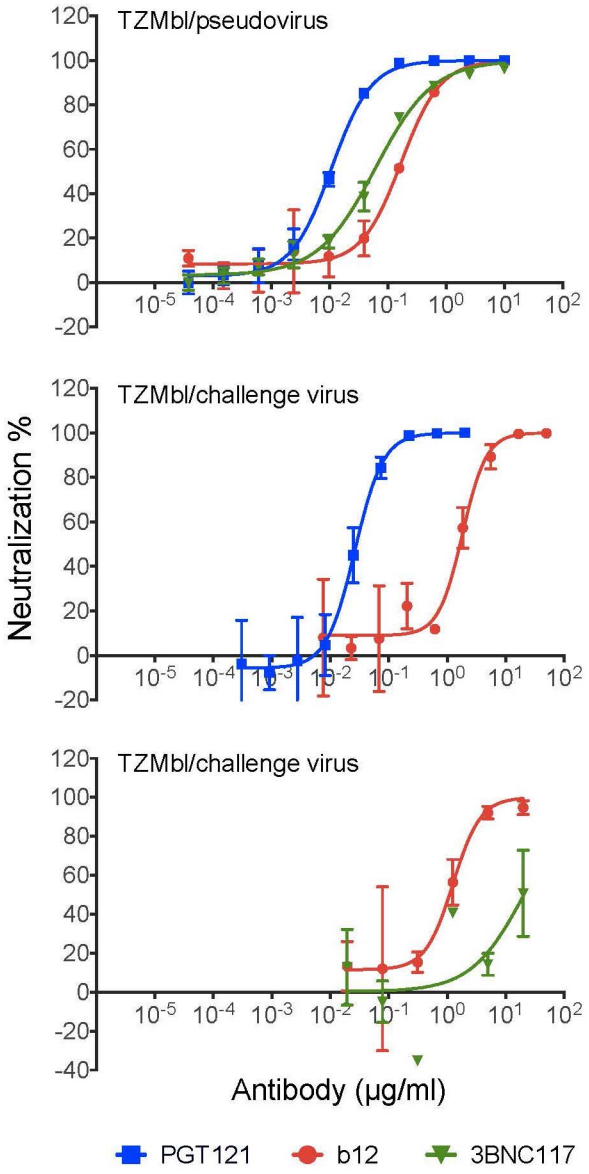

Extended Data Figure 6 | Neutralization sensitivity of SHIV-SF162P3 pseudovirus and our SHIV-SF162P3 challenge stock. TZM-bl neutralization assays of PGT121, 3BNC117 and b12 against the SHIV-SF162P3 pseudovirus (top) and against the SHIV-SF162P3 challenge stock (middle, bottom). Note sensitivity of our SHIV-SF162P3 challenge stock to PGT121 but relative resistance to 3BNC117.

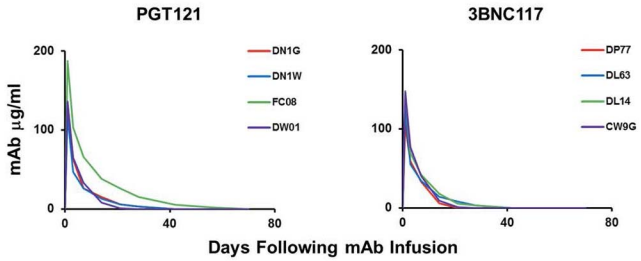

Extended Data Figure 7 | Monoclonal antibody titres after administration of the single monoclonal antibodies PGT121 and 3BNC117. PGT121 and 3BNC117 titres in the monkeys described in Fig. 3 after infusion of the single monoclonal antibodies.

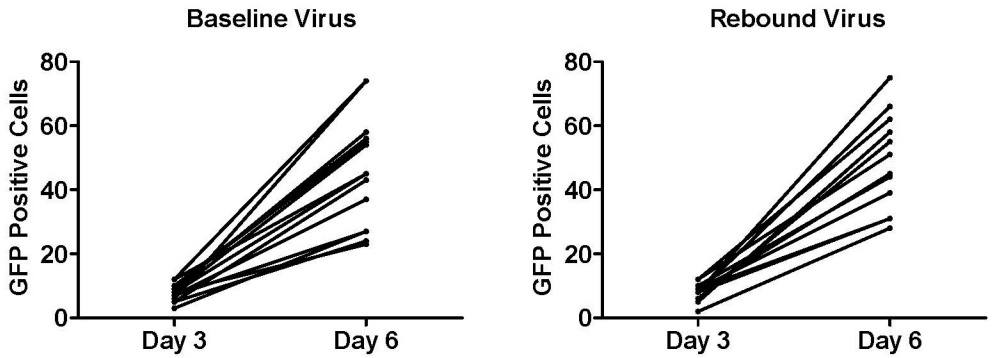

Extended Data Figure 8 | Virus replicative capacity at baseline and following virus rebound. Numbers of GFP-positive infected GHOST indicator cells per well after 3 and 6 days of culture with baseline or rebound SHIV-SF162P3 virus.

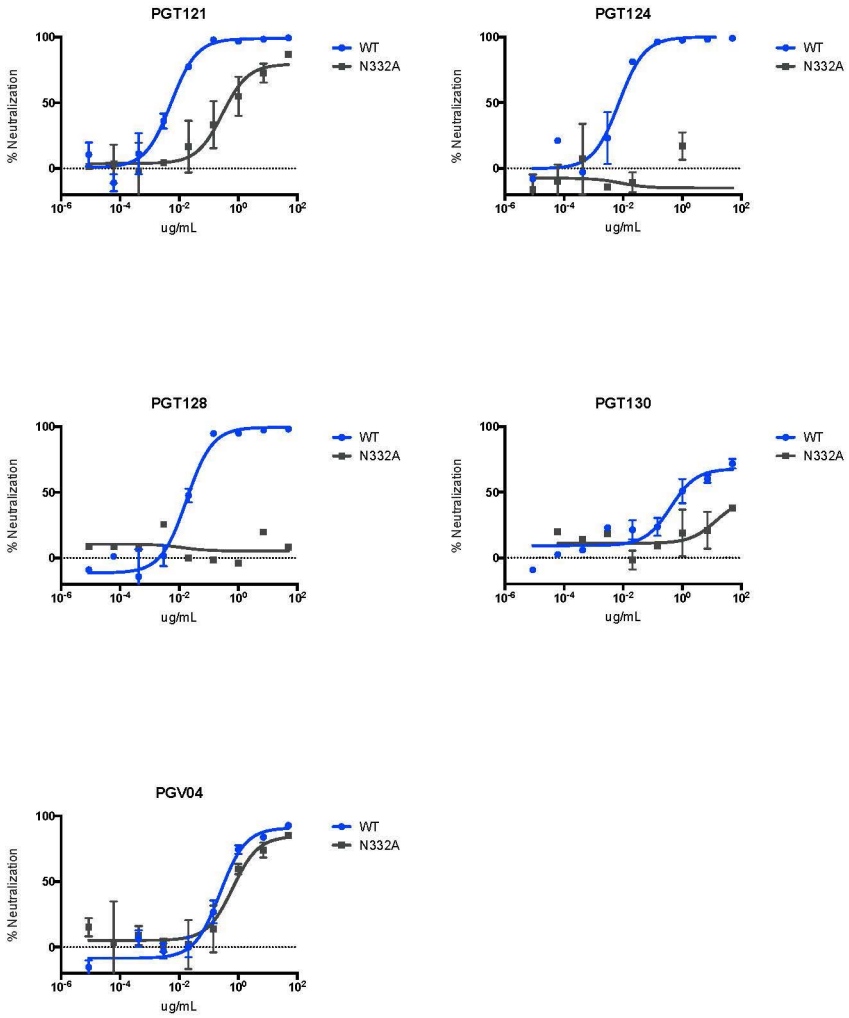

Extended Data Figure 9 | Monoclonal antibody sensitivity to N332A mutated SHIV-SF162P3. TZM-bl neutralization assays of PGT121, PGT124, PGT128, PGT130 and PGV04 against SHIV-SF162P3 containing the N332A mutation. Note 100-fold reduced sensitivity to PGT121 but more profound escape from PGT124 and PGT128.

Extended Data Table 1 | Viral decay kinetics

Therapy	*r* (logs/day)† Median (IQR)	Median $t_{1/2}$ (days)#	Fold decrease in viral load over a 7-day period
DTG + TNF/FTC (SIV/monkeys)	0.229 (0.198-0.265)*	1.31	40
EFV + 2 NRTI (HIV/humans)	0.294 (0.273-0.334)	1.02	112
RAL + TDF/FTC (HIV/humans)	0.264 (0.253-0.284)	1.15	70
PGT121 mAb (SHIV/monkeys)	0.382 (0.338-0.540)	0.78	468

Kinetics of decline of plasma viraemia after antiretroviral therapy in rhesus monkeys and humans and after monoclonal antibody administration in rhesus monkeys. DTG, dolutegravir; EFZ, efavirenz; FTC, emtricitabine; NRTI, nucleoside reverse transcriptase inhibitor; RAL, raltegravir; TDF, tenofovir disoproxil fumarate; TNF, tenofovir.

* Computed using viral load measurements at day 0 and day 12 (J.B.W., unpublished).

† In the case of EFV and RAL therapies, decline rates *r* correspond to the 'first phase' of viral decline. Values reported in ref. 28 have been converted to logs/day (base 10). Note that the specific rate of decline due to RAL is slower than that due to EFV. The rapid viral decline in RAL compared to EFV is due to a longer duration in the first phase and a slower transition into the second phase, where viral decline rates are lower.

#The half-life, $t_{1/2} = \ln(2)/r*\ln(10)$.